Langmuir
Article
pubs.acs.org/Langmuir

Extensive Bilayer Perforation Coupled with the Phase Transition Region of an Anionic Phospholipid

Karin A. Riske,*,† Lia Q. Amaral,‡ and M. Teresa Lamy‡

†Departamento de Biofísica, Universidade Federal de São Paulo, R. Botucatu, 862 CEP 04023-062, São Paulo, SP, Brazil, and ‡Instituto de Física, Universidade de São Paulo, CP 66.318 CEP 05315-970, São Paulo, SP, Brazil

Received April 6, 2009. Revised Manuscript Received May 19, 2009

At low ionic strength dimyristoylphosphatidylglycerol (DMPG) exhibits a broad phase transition region characterized by several superimposed calorimetric peaks. Peculiar properties, such as sample transparency, are observed only in the transition region. In this work we use differential scanning calorimetry (DSC), turbidity, and optical microscopy to study the narrowing of the transition region with the increase of ionic strength (0−500 mM NaCl). Upon addition of salt, the temperature extension of the transition region is reduced, and the number of calorimetric peaks decreases until a single cooperative event at T_m = 23 °C is observed in the presence of 500 mM NaCl. The transition region is always coupled with a decrease in turbidity, but a transparent region is detected within the melting process only in the presence of up to 20 mM NaCl. The vanishing of the transparent region is associated with one of the calorimetric peaks. Optical microscopy of giant vesicles shows that bilayers first rupture when the transition region is reached and subsequently lose optical contrast. Fluorescence microscopy reveals a blurry and undefined image in the transparent region, suggesting a different lipid self-assembly. Overall sample turbidity can be directly related to the bilayer optical contrast. Our observations are discussed in terms of the bilayer being perforated along the transition region. In the narrower temperature interval of the transparent region, dependent on the ionic strength, the perforation is extensive and the bilayer completely loses the optical contrast.

Introduction

Control of cell membrane permeability is fundamental to sustaining life. Lipid bilayers are a natural permeability barrier of cells against polar and charged molecules. Generally, controlled and specific transport across the membrane is done through numerous protein channels and pumps embedded in the lipid bilayer. Alternatively, unspecific increase in lipid bilayer permeability can be induced by strong electric pulses,[1,2] pore-forming peptides/drugs,[3] lipid phase transition,[4−6] or amphiphile insertion.[7] In all of these cases, pores (transient or stable) open across the membrane, allowing molecules to cross. Transport across primitive cells could not rely on complex protein channels and had to depend on some simple mechanism involving lipid bilayers alone.[8]

Lipid bilayer stability relies on the balance of different lipid−lipid interactions. The hydrophobic effect is the main actor in lipid self-assembly. The preferred structure formed, however, depends mainly on the packing properties of the hydrophobic and hydrophilic parts, which are also influenced by interactions among lipids. The presence of membrane surface charges, found in all biological membranes, certainly adds a significant contribution to lipid−lipid interactions. The effective tension applied to the membrane can also destroy its stability, as is the case in electroporation and mechanical lysis.[9] Here we concentrate mainly on the effects of the main phase transition on the stability of a charged phospholipid bilayer. The permeability of lipid membranes exhibits a discontinuity at its main phase transition region because of the formation of transient small pores.[4−6]

The anionic phospholipid dimyristoylphosphatidylglycerol (DMPG) at high ionic strength (above 100 mM NaCl) exhibits a thermal behavior quite similar to that of its zwitterionic analogue DMPC (dimyristoylphosphatidylcholine). At low ionic strength, however, the gel-to-fluid phase transition extends over more than 10 °C, and unique system properties are detected.[10−16] The excess heat capacity profile shows a sequence of several peaks, between a very sharp one, defining the beginning of the melting process ($T_m^{on} \sim 18$ °C), and a broad one, which sets its end ($T_m^{off} \sim 30-40$ °C).[17] The transition region, which has also been termed intermediate phase (IP), has specific characteristics not found in the neighboring phases: an unusually low turbidity,[12,18] high

*Corresponding author: Ph 55 11 5576 4530, Fax 55 11 5571-5780, e-mail kar@biofis.epm.br.

(1) Chernomordik, L. V.; Sukharev, S. I.; Popov, S. V.; Pastushenko, V. F.; Sokirko, A. V.; Abidor, I. G.; Chizmadzhev, Y. A. *Biochim. Biophys. Acta* **1987**, *902*, 360–373.
(2) Riske, K. A.; Dimova, R. *Biophys. J.* **2005**, *88*, 1143–1155.
(3) Matsuzaki, K.; Murase, O.; Fujii, N.; Miyajima, K. *Biochemistry* **1995**, *34*, 6521–6526.
(4) Nagle, J. F.; Scott, H. L.Jr. *Biochim. Biophys. Acta* **1978**, *513*, 236–243.
(5) Antonov, V. F.; Petrov, V. V.; Molnar, A. A.; Predvoditelev, D. A.; Ivanov, A. S. *Nature (London)* **1980**, *283*, 585–586.
(6) Antonov, V. F.; Anosov, A. A.; Norik, V. P.; Smirnova, E. Y. *Eur. Biophys. J.* **2005**, *34*, 155–162.
(7) Heerklotz, H.; Seelig, J. *Biochim. Biophys. Acta* **2001**, *508*, 69–85.
(8) Mansy, S. S.; Schrum, J. P.; Krishnamurthy, M.; Tobe, S.; Treco, D. A.; Szostak, J. W. *Nature (London)* **2008**, *454*, 122–126.
(9) Evans, E.; Rawicz, W. *Phys. Rev. Lett.* **1990**, *17*, 2094–2097.
(10) Epand, R. M.; Hui, S.-W. *FEBS Lett.* **1986**, *209*, 257–260.
(11) Salonen, I. S.; Eklund, K. K.; Virtanen, J. A.; Kinnunen, P. K. J. *Biochim. Biophys. Acta* **1989**, *982*, 205–215.
(12) Heimburg, T.; Biltonen, R. L. *Biochemistry* **1994**, *33*, 9477–9488.
(13) Schneider, M. F.; Marsh, D.; Jahn, W.; Kloesgen, B.; Heimburg, T. *Proc. Natl. Acad. Sci. U.S.A.* **1999**, *96*, 14312–14317.
(14) Lamy-Freund, M. T.; Riske, K. A. *Chem. Phys. Lipids* **2003**, *122*, 19–32.
(15) Riske, K. A.; Fernandez, R. M.; Nascimento, O. R.; Bales, B. L.; Lamy-Freund, M. T. *Chem. Phys. Lipids* **2003**, *124*, 69–80.
(16) Riske, K. A.; Amaral, L. Q.; Döbereiner, H.-G.; Lamy, M. T. *Biophys. J.* **2004**, *86*, 3722–3733.
(17) Riske, K. A.; Amaral, L. Q.; Lamy-Freund, M. T. *Biochim. Biophys. Acta* **2001**, *1511*, 297–308.
(18) Riske, K. A.; Politi, M. J.; Reed, W. F.; Lamy-Freund, M. T. *Chem. Phys. Lipids* **1997**, *89*, 31–44.

electrical conductivity,[18] and high sample viscosity.[12,13] Small-angle X-rays scattering (SAXS) showed that DMPG at low ionic strength is arranged in uncorrelated bilayers and displays a lower electron density contrast in the transition region.[17] Electron spin resonance (ESR) of a spin label located at the bilayer center revealed the coexistence of two structurally different microenvironments in the transition region: one resembling a bilayer with intermediate mobility between a gel and a fluid phase and one with high mobility and fairly hydrated, more compatible with a micelle-like environment.[15] X-rays results at a smaller angle region revealed the existence of a mesoscopic correlation around 370 Å only in the transition region.[16] Optical microscopy of DMPG giant vesicles showed that the bilayers lose its optical contrast in the transition region.[16]

It has been proposed that DMPG at low ionic strength forms a lipid network in the transition region,[13] similar to the so-called sponge phase. This possibility was ruled out based on experiments that discarded lipid rearrangement between DMPG structures along the transition region[14,19] and on SAXS data.[16] Instead, we proposed that in-plane correlated cavities/pores open on the membrane surface, giving rise to the mesoscopic correlation detected by SAXS and decrease of optical contrast.[16] In a following work,[19] it was proposed that opened (tattered) bilayer sheets exist in the transition region and that changes in sodium and proton association in the melting region could be responsible for changes in bilayer curvature.

As the ionic strength is increased, the temperature extension of the transition region is reduced.[11,13,18,20,21] Around 100−500 mM NaCl, the transition region is not detected and the thermal behavior of DMPG resembles that of DMPC, with a single T_m at 23 °C. In pure water and at room temperature, DMPG forms small-sized particles with altered morphology, resembling disks and open shells, as revealed by electron microscopy.[10] At low concentrations of salt, DMPG is organized mainly as uncorrelated bilayers forming submicroscopic structures, most probably vesicles, as seen with optical microscopy and SAXS.[17,21] The SAXS peak around 370 Å at 25 °C disappears with 20 mM NaCl.[21] Above 50 mM NaCl, few giant multilamellar vesicles (MLVs) can be seen, although most lipids are still forming small vesicles. Around 500 mM NaCl, the preferred structures detected with optical microscopy are MLVs, whose lamellae are still poorly correlated, deduced from the faint Bragg peaks in the SAXS data.[21]

Here we present a detailed study of the vanishing of the transition region and of its specific properties with increasing concentrations of salt. On the one hand, DMPG dispersions are studied with DSC and turbidity, giving special attention to changes within the transition region between T_m^{on} and T_m^{off}. On the other hand, new optical and fluorescence microscopy observations of DMPG giant vesicles (uni- and multilamellar) with increasing ionic strength reveal properties of DMPG membranes along the transition region with more detail. We close this work with a discussion of the lipid assembly adopted in the transition region of DMPG.

Materials and Methods

Materials. The sodium salt of the phospholipid DMPG (1,2-dimyristoyl-*sn*-glycero-3-[phospho-*rac*-glycerol]) was purchased from Avanti Polar Lipids (Birmingham, AL). The fluorescent probe $DiIC_{18}$ (1,1′-dioctadecyl-3,3,3′,3′-tetramethylindodicarbocyanine, 4-chlorobenzenesulfonate salt) was from Molecular Probes (Eugene, OR). The buffer system used was 10 mM Hepes (4-(2-hydroxyethyl)-1-piperizineethanesulfonic acid) adjusted with NaOH to pH 7.4. Milli-Q water was used throughout.

Lipid Dispersion Preparation. A lipid film was formed from a chloroform solution, dried under a stream of N_2 and left under reduced pressure for a minimum of 2 h, to remove all traces of the organic solvent. Dispersions were prepared by the addition of the Hepes buffer with different concentrations of salt (from 0 up to 500 mM NaCl), followed by vortexing for about 2 min above T_m^{off} (~40 °C). The samples were kept at room temperature and used right after preparation.

Differential Scanning Calorimetry. The calorimetric data were carried out in a Microcalorimeter VP-DSC (MicroCal, Northampton, MA) at a scan rate of 10 °C/h. Baseline subtractions and peak integrals were done using the MicroCal Origin software with the additional module for DSC data analysis provided by MicroCal.

Turbidity Measurements. Sample turbidity (absorbance at λ = 350 nm and 2 mm optical path) was measured on 50 mM DMPG in 10 mM Hepes pH 7.4 with the addition of 0 to 500 mM NaCl with a HP 8452 A diode array spectrophotometer (Hewlett-Packard Co., Palo Alto, CA). Temperature was adjusted with a circulating water bath and measured inside the sample with a thermocouple. Generally, the temperature was increased in 2 °C steps and sample was allowed 15 min of equilibration time before each measurement.

Optical Microscopy. Giant multilamellar vesicles (MLVs) of 50 mM DMPG containing 1 mol % $DiIC_{18}$ were prepared at 30 °C as described above in the section Lipid Dispersion Preparation. The aqueous solution used contained 10 mM Hepes pH 7.4, 0.5 mM EDTA, and 500 mM NaCl. This vesicle dispersion was then diluted 250× in 10 mM Hepes pH 7.4 + 0.5 mM EDTA containing different concentrations of NaCl to yield a final 0.4 mM DMPG in concentrations of salt ranging from 2 to 25 mM NaCl. The dilution was performed at ~10 °C (with the lipids in the gel phase), and the dispersion was immediately transferred into an observation chamber with temperature control set at 16 °C, so that the lipids remained in the gel phase. The observation chamber was connected to a water circulating bath and temperature inside the observation chamber was checked with a thermocouple. Giant MLVs deposited on the coverslip due to gravity, so the local lipid concentration was higher. The vesicles were observed with a Ph2 63× objective in an inverted Zeiss Axiovert 200 (Jena, Germany) equipped with a digital camera Zeiss AxioCam HSm (Jena, Germany).

Results

Differential Scanning Calorimetry and Turbidity of DMPG Dispersion. Figure 1a shows a series of DSC traces obtained with 50 mM DMPG at increasing concentrations of salt between 0 and 500 mM NaCl. At very high ionic strength (500 mM NaCl) a very sharp and intense peak associated with the chain melting transition is detected at T_m = 23 °C, similar to DMPC.[22] Note that the traces obtained at high ionic strength are reduced in respect to those obtained at lower ionic strengths. As the salt concentration is decreased, the single T_m peak is replaced by a gradually wider transition region, comprising an increasing number of peaks. A relatively sharp peak, defining the onset of the transition, T_m^{on}, still marks a cooperative beginning of the melting process, and a broad peak at T_m^{off} indicates the end of the melting region (T_1, T_2, and T_3 marked in Figure 1a will be discussed later). Around 10−14 °C, all curves show a pretransition peak, T_p,

(19) Alakoskela, J.-M. I.; Kinnunen, P. K. J. *Langmuir* **2007**, *23*, 4203–4213.
(20) Riske, K. A.; Döbereiner, H.-G.; Lamy, M. T. *J. Phys. Chem. B* **2002**, *106*, 239–246.
(21) Fernandez, R. M.; Riske, K. A.; Amaral, L. Q.; Itri, R.; Lamy, M. T. *Biochim. Biophys. Acta* **2008**, *1778*, 907–916.
(22) Lewis, R. N. A. H.; Mak, N.; McElhaney, R. N. *Biochemistry* **1987**, *26*, 6118–6126.

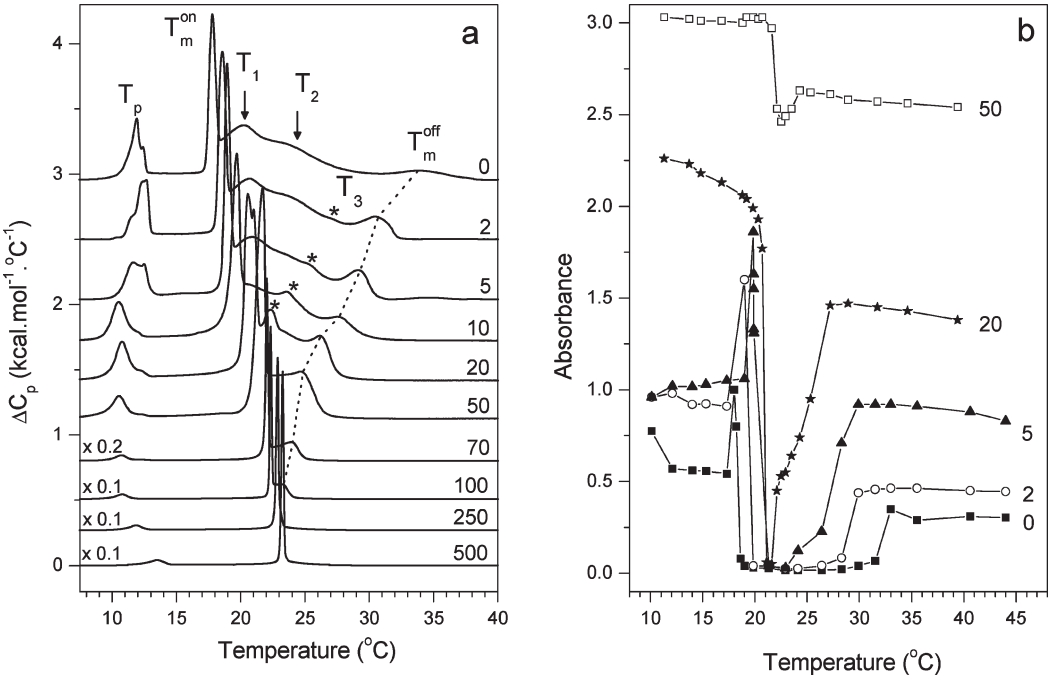

Figure 1. (a) Excess heat capacity (ΔC_p) of 50 mM DMPG in 10 mM Hepes pH 7.4 with different concentrations of salt (indicated on the right in mM). The curves were shifted for clarity. The curves at high ionic strength (70−500 mM NaCl) were reduced (indicated on the left). The scan rate was 10 °C/h. The various transition temperatures are indicated on the top. Arrows mark the position of T_1 and T_2 in the first trace. The positions of T_3 and T_m^{off} are indicated with asterisks and a dotted line, respectively. (b) Absorbance measured at 350 nm with a 2 mm optical path of some of the same samples in (a). The turbidity profiles in the presence of 10 and 70 mM NaCl (not shown) resemble that of 5 and 50 mM NaCl, respectively. Above 50 mM NaCl the turbidity of the dispersion is already beyond the absorbance sensitivity, and only the general profiles are reliable.

associated generally with a transition to a ripple phase.[23,24] The position and enthalpy of the pretransition change slightly with the concentration of salt, but this will not be discussed in the present work. The enthalpy of the whole transition region (between T_m^{on} and T_m^{off}) is basically the same for all conditions ($\Delta H \sim 5$ kcal/mol).

One of the most characteristic features of the transition region of DMPG at low ionic strength is the sample transparency.[12,18] Figure 1b shows turbidity measurements of some of the samples used in the DSC experiment. Visual transparency corresponds to absorbance practically at the zero level (below ~0.06 in our setup). The data show that a transparent region between the (turbid) gel and fluid phases exists only in the presence of up to 20 mM NaCl. In the presence of 50−70 mM NaCl, sample turbidity shows a minimum associated with the region between T_m^{on} and T_m^{off}, but the sample is visually turbid in all temperature range. Above 100 mM NaCl, a small decrease in turbidity accompanies the phase transition.[18] Indeed, as the ionic strength is increased above 50 mM NaCl, more and more multilamellar structures are formed,[21] which are responsible for the large increase in sample turbidity.

Let us now focus on the range of low ionic strength (0−20 mM NaCl), for which a transparent region exists and several calorimetric peaks are detected with DSC, shown in more detail in Figure 2a. The sequence of superimposed calorimetric peaks of DMPG, though complex, is characteristic for each salt condition. Here we try to follow each peak as the ionic strength is increased. Up to now we have been mainly concerned with the two outermost peaks, namely T_m^{on}, the sharp peak that triggers the whole process, and T_m^{off}, which sets its end. Upon the increase in ionic strength, T_m^{on} shifts to higher temperatures whereas T_m^{off} shifts to lower temperatures. The intermediate peaks are at first sight not so easy to follow as the ionic strength is increased. However, from the turbidity data between 5 and 20 mM NaCl, we conclude that the transparent region is narrower than the whole transition region, finishing with a first increase in turbidity at a temperature below T_m^{off}. This first increase in turbidity can be associated with the small calorimetric peak marked with an asterisk in Figures 1a and 2a and termed T_3. Figure 2b shows the comparison of DSC and turbidity data obtained for the same sample at 10 mM NaCl, showing evidence for the correlation between the first increase in turbidity and the calorimetric peak at T_3. This peak is first detected at 5 mM NaCl and becomes more pronounced with the increase of salt. At 2 mM NaCl a very small calorimetric peak, assigned to T_3, is detected, associated with a minute increase in turbidity. For intermediate concentrations of salt (5−20 mM NaCl), the transparent region thus exists only between T_m^{on} and T_3.

After the identification of T_3, the other peaks between T_m^{on} and T_m^{off} could be easily followed with the increase in ionic strength and were termed T_1 and T_2 (see Figures 1a and 2a). T_1 increases slightly with the increase of salt, becomes narrower at 20 mM NaCl, and vanishes (or collapses with T_m^{on}) at 50 mM NaCl. The peak at T_2 is observed only up to 5 mM NaCl, but this peak seems to underlie the other peaks at higher ionic strengths, hardly changing its position, which coincides with the final T_m value reached at 500 mM NaCl. No changes in turbidity correlated with T_1 and T_2 were detected. The thermal events associated with these peaks will not be discussed here.

With the identification of the several calorimetric peaks, we can now describe the whole transition region as follows. A critical increase in turbidity occurs around T_m^{on} up to 10 mM NaCl, as was previously reported with 2 mM NaCl.[16] This turbidity

(23) Tardieu, A.; Luzzati, V.; Reman, F. C. *J. Mol. Biol.* **1973**, *75*, 711–733.
(24) Riske, K. A.; Barroso, R. P.; Vequi-Suplicy, C. C.; Germano, R.; Henriques, V. B.; Lamy, M. T. *Biochim. Biophys. Acta* **2009**, in press.

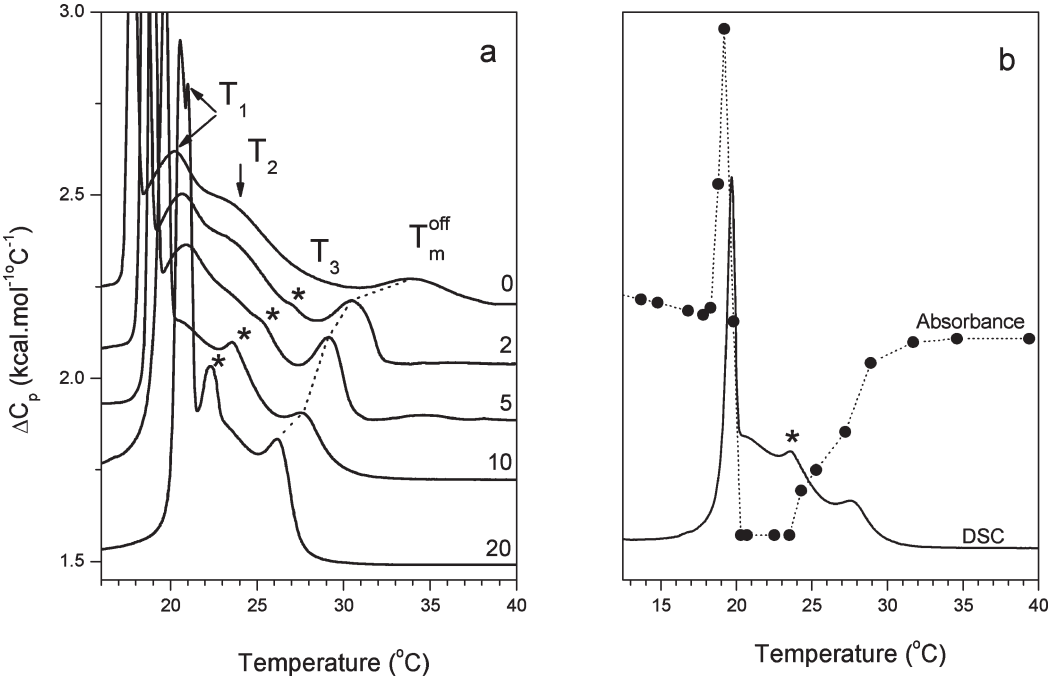

Figure 2. (a) Magnified region of Figure 1a. DSC traces of 50 mM DMPG in the presence of 0-20 mM NaCl. (b) Comparison between DSC and turbidity data for 50 mM DMPG in the presence of 10 mM NaCl.

increase around T_m^{on} is probably related to typical peak anomaly due to structural phase transitions and long-range correlation.[25] At 20 mM NaCl the sharp increase in turbidity is no longer detected. The turbidity decreases abruptly concomitantly with the calorimetric peak at T_m^{on}. The partial recovery of turbidity in the fluid phase seems to be achieved in two steps at intermediate ionic strength. A first increase in turbidity occurs at T_3, being more pronounced the narrower the peak at T_3 becomes with the increase of salt. A second increase in turbidity occurs at T_m^{off}, restoring the turbidity almost to its value in the gel phase, correlating with the end of the melting process. The visually transparent region exists for all samples only between T_m^{on} and T_3, persisting up to T_m^{off} in the very low ionic strength conditions (0−2 mM NaCl). Between 50 and 70 mM NaCl, only three peaks are detected in the DSC traces: T_m^{on}, T_2, and T_m^{off}. The samples are visually turbid for all temperature range, though a minimum in turbidity is observed along the transition region. At higher concentrations of salt (above 100 mM NaCl), a small decrease in turbidity coupled with T_m (or T_m^{on}) is observed. This is the expected behavior of a conventional gel−fluid transition, seen for instance with DMPC.[18]

Optical Microscopy of Giant DMPG Vesicles. Giant unilamellar vesicles (GUVs) are usually prepared with the standard electroformation method.[26] This method is widely used to grow GUVs made of neutral or mixtures of neutral and charged lipids. However, GUVs are not readily prepared from pure charged lipids using electroformation (few small-sized vesicles are observed after the usual electroformation protocol). In a previous work, we could prepare GUVs of DMPG using this methodology, but only when electrode wires were placed inside the observation chamber above 40 °C.[16] Here we use an alternative approach to obtain giant vesicles. At 50 mM DMPG and very high ionic strength (500 mM NaCl), the interbilayer repulsion is screened and DMPG spontaneously forms giant multilamellar vesicles (MLVs) of 1−10 μm diameter, large enough to be individually observed with optical microscopy.[21] These MLVs are stable, even if the main transition (a single event at 23 °C; see Figure 1a) is crossed several times. Once formed, the MLVs were diluted in a buffer solution containing different concentrations of salt, thus yielding 0.4 mM DMPG at defined concentrations of salt, between 2 and 25 mM NaCl. When the dilution was performed in the gel or fluid phase, the MLVs were stable within at least 1 h. However, when the transition region was reached (either from the gel or from the fluid phase) the MLVs ruptured and disassembled and were irreversibly destroyed. This disassembly was not caused by osmotic stress due to the dilution protocol, as will be discussed later. When the temperature was increased to the fluid phase, giant (mainly unilamellar) vesicles spontaneously formed.

The optical microscopy observations on the processes described above will be divided in two parts. First, we will follow one MLV through the transition region and discuss this particular case. Afterward, we will show temperature cycles of GUVs (obtained after MLVs disassembly in the transition region) at different ionic strengths, both with phase contrast and fluorescence microscopy.

Figure 3 shows an example of one MLV (obtained after dilution of MLVs in the gel phase to yield a final concentration of salt of 2 mM NaCl) during the first heating scan. Around 20 °C (Figure 3b) the multilamellar structure first swells and then "burst" within seconds, through pealing off of several layers (see Figure 3c,d). This temperature is slightly higher than T_m^{on} for this ionic strength (18.6 °C, Figure 1), probably because of the initially entrapped salt in the multilamellar structure. Afterward, the optical contrast of the individual bilayers decreases (22−25 °C, Figure 3e,f) until nothing is detected with phase contrast (Figure 3f,g). The decrease in bilayer optical contrast in the transition region was already observed in a previous work.[16] With further increase in temperature, the bilayer optical contrast is regained around 26 °C (Figure 3h,i), and the bilayers,

(25) Cummins, H. Z.; Levanyuk, A. P. *Light Scattering Near Phase Transitions*; North-Holland: Amsterdam, The Netherlands, 1983.
(26) Angelova, M. I.; Dimitrov, D. S. *Faraday Discuss. Chem. Soc.* **1986**, *81*, 303–311.

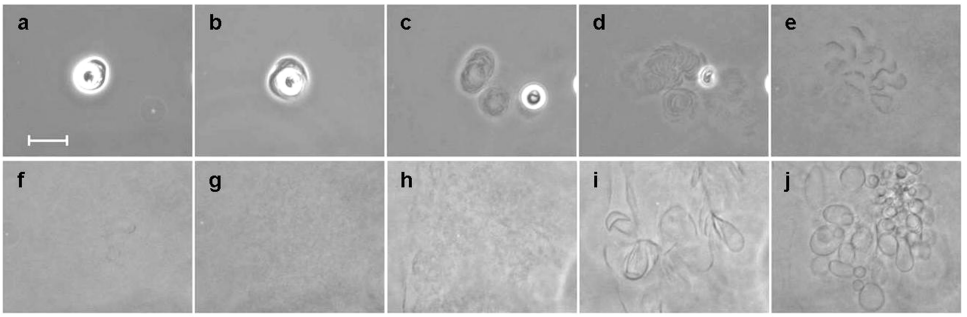

Figure 3. Phase contrast microscopy images of a MLV formed at high ionic strength and diluted in pure buffer to yield a final 2 mM NaCl concentration of salt. The sequence shows a heating scan: (a) 17, (b) 20, (c−e) 21, few seconds apart, (f) 22, (g) 25, (h) 26, (i) 26.5, and (j) 28 °C. The whole heating scan lasted around 40 min. The scale bar corresponds to 20 μm.

previously engaged in forming a single MLV, reseal into numerous single vesicles, mainly giant unilamellar vesicles (around 28 °C, Figure 3j). The dense multilamellar structure is irreversibly lost. The same disintegration mechanism is seen if the MLVs dilution is performed in the fluid phase, and an individual MLV is observed upon cycling through the transition region (not shown).

It is worth stressing that the MLV disruption/disappearance shown in Figure 3 is indeed associated with the specific properties of DMPG displayed only in a low ionic strength range (2−20 mM NaCl) and is not an artifact due to the dilution protocol. The effect of osmotic stress on MLVs integrity was examined in the following way. First, MLVs of the neutral lipid DMPC were prepared and diluted in the same way, creating the same osmotic difference as with DMPG (500 mM NaCl inside, no salt outside). The DMPC MLVs kept their integrity even when crossing the phase transition. Thus, osmotic stress alone cannot be responsible for the disruption observed. Second, the dilution of MLVs of DMPG in 500 mM NaCl was done in an equiosmolar (salt-free) solution containing 1 M glucose. The same MLV disruption was observed when the transition region was reached. This proves that the disruption is also observed when no osmotic difference is present across the bilayer. To check the effect of the large interlayer repulsion on MLV stability, MLVs of DPPG, which bears the same headgroup as DMPG but with longer chains, were prepared in the same way. DPPG is known to hardly display anomalies associated with the phase transition[13] and to form multilamellar structures only above 300 mM NaCl.[27] No disruption effect was observed upon crossing the main transition of DPPG after dilution in salt-free equiosmolar buffer. Thus, the disruption of MLVs observed with DMPG at low ionic strength (Figure 3) is correlated with the specific properties of this lipid.

Similar heating scans as shown in Figure 3 were obtained for several MLVs diluted to the final concentration of salt between 2 and 25 mM NaCl. The vesicle behavior with increasing ionic strength described in the following was observed in several vesicles at the same condition, either as an ensemble in the same observation field or in different experiments. As the ionic strength was increased from 2 to 20 mM NaCl, the temperature interval where the bilayer remained transparent under the microscope decreased. This temperature interval coincided with the transparent region observed from the turbidity results on DMPG dispersions for each concentration of salt (Figure 1b). The temperatures when the bilayers regained their contrast (see Table 1) decreased with the increase in the concentration of salt and coincided reasonably well with T_3 (Figures 1 and 2). The vesicle reforming process generally finished at a temperature close to T_m^{off}. The extent of MLVs disintegration was dependent on the ionic strength. Between 2 and 10 mM NaCl, the disintegration was generally complete, and mainly unilamellar vesicles were seen in the fluid phase. On the other hand, between 15 and 20 mM NaCl, the transparent window was very narrow in temperature (1−2 °C), and some multilamellar vesicles, though less dense than in the gel phase, were still observed in the fluid phase. Above 25 mM NaCl the bilayers never became transparent, although the MLVs partly disassembled between T_m^{on} and T_m^{off}. At higher ionic strengths (above 50 mM NaCl), the MLVs preserved their integrity when the main transition was crossed.

Table 1. Transition Temperatures[a]

	microscopy		turbidity		DSC	
[NaCl] (mM)	T_3 (°C)	T_m^{off} (°C)	T_3 (°C)	T_m^{off} (°C)	T_3 (°C)	T_m^{off} (°C)
2	25	∼28−32	27[b]	29.0	27.0	30.4
5	24	28	25.0	27.5	24.4	29.2
10	23	26	24.0	27.0	23.6	27.6
15	22	23				
20	21	22	21.9	24.8	22.4	26.2
25		22				

[a] The column labeled Microscopy shows transition temperatures determined from observation of giant vesicles (uni- and multilamellar) in different concentrations of salt. T_3 was determined from the recovery/loss of the bilayer optical contrast under phase contrast, which is concomitant with the definition of a sharp image bilayer in fluorescence mode. T_m^{off} was determined from morphological changes of vesicles accompanied by change in bilayer contrast (down scan) and from complete vesicle resealing (up scan). Each vesicle in an observation field shows the transitions events at a slightly different temperature (within 1−2 °C). The columns labeled Turbidity and DSC list the transition temperatures obtained from the data shown in Figure 1. [b] Detected as a minute increase in turbidity.

It is interesting to call the attention to the difference in cycling a multilamellar and a unilamellar giant vesicle through the transition region. In the latter case, the same vesicle can be obtained after the temperature cycle (as shown previously[16] and later here), whereas multilamellar vesicles are always irreversibly destroyed (especially below 10 mM NaCl). The main difference between the two cases is that the bilayers experience a strong interlayer repulsion within the MLVs, which are not any longer in the screening conditions in which they were formed. In the gel and fluid phases, the bilayer cohesion is strong enough to keep the MLVs stable. On the other hand, the bilayers in the transition region are prone to getting destabilized, allowing for the interlayer repulsion to act. Thus, the evident increase in interbilayer distance observed in Figure 3 (see sequence of snapshots b−e) when the MLV enters the transition region seems to be caused by the strong electrostatic repulsion among the bilayers. When the fluid phase is then reached, the bilayers that formed a single MLV became

(27) Degovics, G.; Latal, A.; Lohner, K. *J. Appl. Crystallogr.* **2000**, *33*, 544–547.

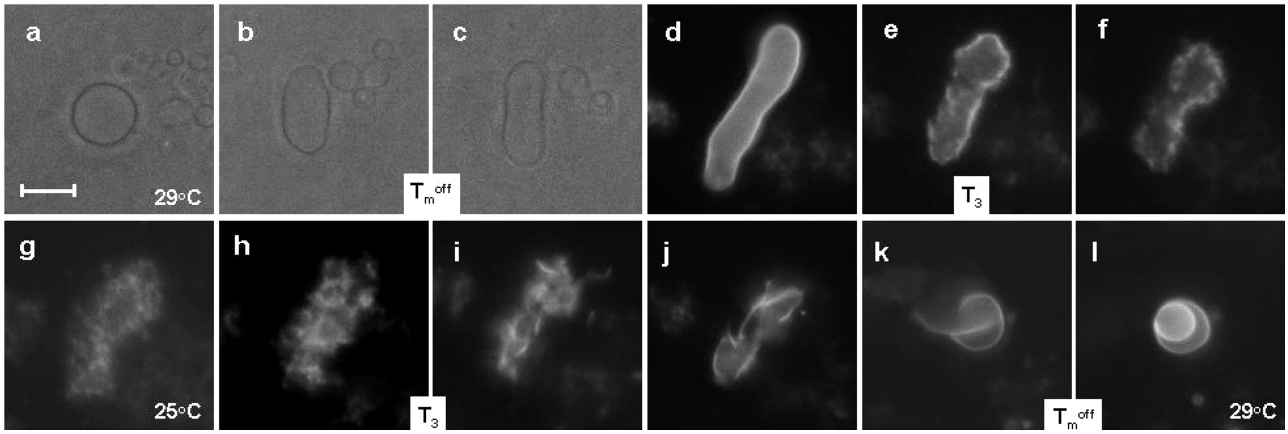

Figure 4. Phase contrast (a−c) and fluorescence microscopy (1 mol % $DiIC_{18}$) (d−l) images of a GUV in Hepes buffer with 5 mM NaCl obtained from a temperature cycle through the transition region ($T_m^{off} \sim 27-28$ °C and $T_3 \sim 25-26$ °C): (a) 29.0, (b) 27.5, (c) 27.0, (d) 26.0, (e) 25.6, (f) 25.5, (g) 25.0, (h) 25.8, (i) 27.0, (j) 27.3, (k) 28.0, and (l) 29.0 °C. The scale bar represents 10 μm. The contrast of the snapshots was enhanced.

uncorrelated and too far apart to reassemble in the original structure, and several unilamellar vesicles are formed instead.

The results shown with MLVs at low ionic strength are certainly very interesting and a manifestation of the particular properties of DMPG. However, the observation of GUVs is definitely a better defined condition, and a closer system to spontaneously formed DMPG dispersions, which do not form multilamellar structures at low ionic strength[21] and most probably form submicroscopic unilamellar vesicles.[13] Furthermore, after MLVs disruption and later formation of GUVs, no relevant asymmetries between the solutions across the bilayers are left.

We now present the results obtained with temperature cycles on GUVs in the presence of intermediate concentrations of salt, for which a transparent region was observed with turbidity measurements (Figure 1b). As already described before,[16] GUVs lose their optical contrast in the transition region but reappear when the lipids return to the fluid phase. The new results of the present study show also fluorescence microscopy images and a more detailed study on the effect of varying the ionic strength. In fact, we conclude that the optical contrast is partially recovered already at T_3, thus below a complete fluid phase. The effects of T_3 and T_m^{off} on GUVs were followed in different vesicles and in different preparations in the presence of 2−20 mM NaCl (see transition temperatures extracted from observations in Table 1), and some examples will be presented and discussed below.

Figure 4 shows a temperature cycle of a GUV through the transition region starting and finishing in the fluid phase. When decreasing the temperature from the fluid phase, we distinguish two different events, which we associate with T_m^{off} and T_3, respectively. The first three snapshots (Figure 4a−c) were obtained with phase contrast mode and the following with fluorescence microscopy, which enables visualization of the bilayer when the optical contrast is lost in the transparent region. The first snapshots (Figure 4a−d) show the effect of crossing T_m^{off} from above. The vesicle elongates significantly (the ratio between the semiaxes increases 5 times) as a result of an increase in the area-to-volume ratio (a rough estimate based on the vesicle projected area shows that the surface area increases around 50% whereas the volume remains roughly constant). Furthermore, the bilayer contrast is reduced, although this will become clearer in a next sequence of snapshots. As the temperature is further decreased, the second event (T_3) starts. The bilayer is ruptured at several places (see Figure 4e,f), suggesting the opening of pores large enough to be visualized with optical microscopy (~1 μm). Below T_3 a blurred and undefined image is detected (Figure 4g). At this point the bilayer is transparent under phase contrast (not shown). When the temperature is again increased to above T_3, bilayer pieces start to become sharp again (Figure 4i−k). These bilayer pieces can also be visualized with phase contrast (similar to Figure 3i). A closed vesicle is observed again only above T_m^{off}, in the fluid phase (Figure 4l). After the cycle, the vesicle changed its structure. It started as a single unilamellar vesicle (Figure 4a) and finished as two vesicles, the smaller trapped inside the bigger (Figure 4l). Quite frequently, the exact same vesicle could not be obtained after one cycle through the transparent region. Note that when decreasing the temperature, the vesicle structure is kept until T_3, whereas in the heating scan a closed surface is recovered only above T_m^{off}.

We now show two other examples of temperature cycles of GUVs through each of the two thermal events separately, T_3 and T_m^{off}. Figure 5 shows a temperature cycle of a GUV through the loss/recovery of bilayer contrast at T_3, observed with fluorescence microscopy. In this example the vesicle seems to be entirely preserved after the cycle. As the temperature decreases, the bilayer is again clearly disrupted at several places (Figure 5b), and a blurry image is observed with further decrease in temperature (Figure 5c,d). When the temperature is increased back, the membrane becomes sharp again (Figure 5e,f) and eventually a homogeneous closed surface is obtained (Figure 5g,h). The fluorescence microscopy images definitely show that the lipids engaged in forming the original vesicle is somehow kept together during the transition region, even though no sharp bilayer can be identified. The lipid assembly that could originate such images will be discussed in the next section.

Figure 6 shows a collection of GUVs during one cycle through T_m^{off}. In the beginning (Figure 6a) and the end (Figure 6h) of the cycle, in the fluid phase, the vesicles are mainly spherical (follow the three biggest vesicles marked with numbers in each snapshot). When the temperature is decreased below T_m^{off}, the vesicles elongate and their bilayer become fainter (see Figure 6a−d). These changes are reversed when the temperature is increased back to above T_m^{off} (see Figure 6d−h).

Such temperature cycles were done with GUVs at different ionic strengths. Basically, the same behavior as shown in Figures 4−6 was observed, with T_3 and T_m^{off} decreasing with the ionic strength, as expected (see Table 1). However, each vesicle in the observation field lost and/or recovered its structure at slightly different temperatures (variations within 1−2 °C). The morphological changes

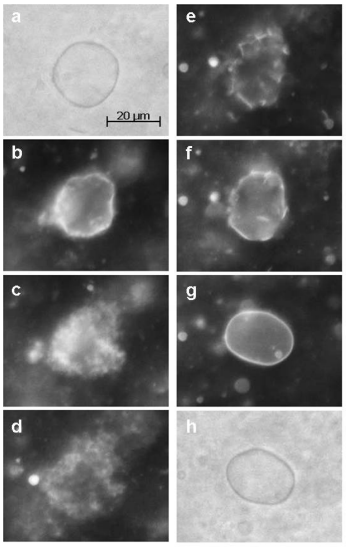

Figure 5. Phase contrast (a, h) and fluorescence microscopy (1 mol % $DiIC_{18}$) images (b−g) of a GUV in Hepes buffer with 2 mM NaCl. The sequence shows a temperature cycle through $T_3 \sim 25$ °C: (a−d) 25.4−24.7 °C; (e−h) 25−26 °C. The contrast of the snapshots was enhanced.

at T_m^{off} (down scan) were only observed with vesicles in the presence of 5−20 mM NaCl (see Table 1), for which a two-step increase in turbidity was detected from the transparent region into the fluid (turbid) phase (Figures 1b and 2b). However, the vesicle elongation and decrease in contrast was less pronounced as the ionic strength was increased.

It is important to mention that the transition temperatures are also somewhat sensitive to the lipid concentration,[12] especially at low ionic strength.[28] Thus, a complete agreement between the transition temperatures obtained with DSC and turbidity (50 mM DMPG) and optical microscopy (0.4 mM DMPG, but concentrated on the coverslip surface; see Materials and Methods) is not to be expected.[28] However, the temperature interval where the bilayer optical contrast vanished under optical microscopy corresponds reasonably well to the transparent region in the turbidity measurements (Table 1 and Figure 1b). The only significant difference (~2 °C) was found at the lowest ionic strength condition (2 mM NaCl), which is more sensitive to changes in lipid concentration.[28] Moreover, the events associated with T_3 (loss/recovery of bilayer contrast under the microscope) were also observed in giant vesicles in the presence of 2 mM NaCl, at a similar

(28) DSC traces of 1 mM DMPG in 10 mM Hepes pH 7.4 + 0.5 mM EDTA with 2, 5, 10, 20, and 50 mM NaCl were obtained for comparison (not shown). In the presence of 2 and 5 mM NaCl the transition temperatures were significantly different from those shown in Figure 1a for 50 mM DMPG. The peak at T_3 could not be detected, whereas T_m^{off} was significantly higher (40.7 and 33.1 °C for 2 and 5 mM NaCl, respectively). In the presence of 10−50 mM NaCl the transition temperatures found with 1 mM DMPG were quite similar to those obtained with 50 mM DMPG. A more detailed study of the behavior of DMPG as a function of lipid concentration is currently under work. For the results discussed here, we see a very good agreement between the transition temperatures obtained with 50 mM DMPG dispersions and optical observations of MLVs diluted from 50 mM DMPG for salt concentrations between 5 and 25 mM NaCl. Although the concentration of DMPG after dilution should be 0.4 mM, the observation is done on a significantly more concentrated region due to (i) precipitation of vesicles on the coverslip surface and (ii) to the fact that the unilamellar vesicles are formed from the disassembly of one MLV and are thus very close to each other. Consequently, we can directly compare the optical microscopy observations done on 5−25 mM NaCl to the DSC and turbidity data performed on dispersions of 50 mM DMPG. At the lowest ionic strength condition (2 mM NaCl), the observations done with optical microscopy suggest that the actual local lipid concentration lies somewhere between 1 and 50 mM. This point should be clarified in the future.

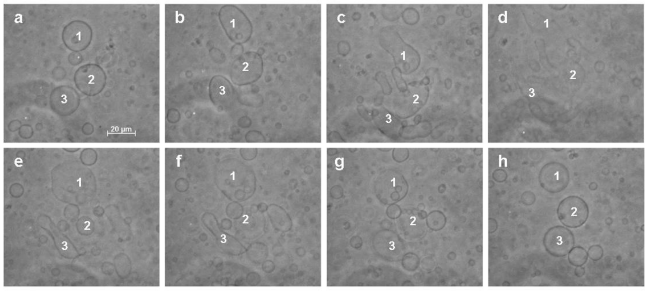

Figure 6. Phase contrast microscopy images of a GUV in Hepes buffer with 5 mM NaCl. The sequence shows a temperature cycle through $T_m^{off} \sim 27$−28 °C: (a) 28.6, (b) 28.2, (c) 27.8, (d) 26.8, (e) 27.2, (f) 27.5, (g) 28.3, and (h) 29.3 °C. The three main vesicles of this ensemble are marked with 1, 2, 3 (vesicle 2 is out of focus in panels e−g). The contrast of the snapshots was enhanced.

temperature to the very small DSC peak assigned to T_3 (see Figure 2a). However, the turbidity data show only a minute increase in turbidity at this temperature (Figure 1b). Even though, we can generally associate the transparent region to the low optical contrast of the bilayer itself.

We also observed the effect of decreasing the temperature to below T_m^{on}, to reach the gel phase. According to the turbidity results (Figure 1b), the dispersion turbidity is highest in the gel phase (even higher than in the fluid phase). The optical microscopy images obtained after cooling vesicles in the presence of 2−20 mM NaCl to around 16 °C show that the bilayer contrast is recovered in the gel phase, but no defined homogeneous vesicles could be detected (see Figure 1 in the Supporting Information). According to electron microscopy data,[13] DMPG forms vesicles in both gel and fluid phases. From our optical microscopy images, DMPG forms vesicles in the fluid phase, but it is not possible to conclude whether closed structures (vesicles with a very rough surface) are obtained in the gel phase. We should call the attention to the difference in vesicle sizes obtained with the two methods and to the fact that bilayers in the gel phase have a much higher bending stiffness and significant resistance to shearing as compared to fluid bilayers.[29,30] Thus a gel phase bilayer in the micrometer length scale might not be able to regain its original structure completely (see Discussion section). If the temperature is increased again, giant vesicles are observed in the fluid phase (second snapshot in Figure 1 in Supporting Information).

Discussion

Transition Region Interval. The phase transition region of DMPG at low ionic strength, which has been previously termed intermediate phase (IP), displays several interesting features not yet fully understood, such as sample transparency and high viscosity. At very low ionic strength, these features are observed in the whole transition region (between T_m^{on} and T_m^{off}).[17,18] However, the DSC traces clearly show the presence of well-defined and reproducible peaks between T_m^{on} and T_m^{off}. The data obtained here show that at intermediate concentrations of salt (5−20 mM NaCl, for 50 mM DMPG) the transparent region exists in a narrower temperature interval, namely between T_m^{on} and T_3, a new thermal event below T_m^{off} detected here with different techniques. When the temperature is increased from the transparent region, we observe a partial recovery of sample turbidity and bilayer optical contrast under the microscope,

(29) Dimova, R.; Pouligny, B.; Dietrich, C. *Biophys. J.* **2000**, *79*, 340–356.
(30) Dimova, R.; Aranda, S.; Bezlyepkina, N.; Nikolov, V.; Riske, K. A.; Lipowsky, R. *J. Phys.: Condens. Matter* **2006**, *18*, S1151–S1176.

events correlated with the small calorimetric peak at T_3. Other properties previously associated with the whole transition region seem also to vanish at T_3, when it is detected below T_m^{off}. Recent SAXS results on 50 mM DMPG with addition of salt[20] revealed that the low angle peak, previously associated with the whole transition region, is well-defined at 25 °C in pure buffer (without salt), becomes broader with addition of 2−10 mM NaCl, and disappears at 20 mM NaCl. Therefore, the emergence of the lower angle SAXS peak only correlates with the transparent region and not with the whole transition region. Even though it was not emphasized before, viscosity data also show that the highly viscous phase finishes concomitantly with the peak at T_3, although the sample still displays a higher viscosity up to T_m^{off} (see Figure 1 in ref 13). Thus, we conclude that the main characteristics previously supposed to exist in the whole transition region, such as sample transparency, loss of bilayer optical contrast, high viscosity, and the presence of a low-angle SAXS correlation peak, are observed only between T_m^{on} and T_3, which we call here the transparent region. However, the transparent region persists up to T_m^{off} at very low ionic strength, when T_3 is not detected and might be collapsed with T_m^{off}.

Another important outcome of our results is the correlation of sample turbidity, measured on DMPG dispersions, and bilayer optical contrast, assessed with optical microscopy of giant vesicles. This was mentioned in our previous work,[16] but it is reinforced here with the more detailed observations at T_3 and T_m^{off}. We show that the bilayer optical contrast vanishes between T_m^{on} and T_3, coinciding with the transparent region, whereas it is partially recovered between T_3 and T_m^{off}, concomitant with a first increase in sample turbidity. Thus, we conclude that sample turbidity is mainly reflecting changes in the bilayer optical contrast. In the following we will discuss how such a loss in bilayer optical contrast can be achieved.

Bilayer Perforation Model. We have proposed before that the transparent region of DMPG at low ionic strength consists of in-plane correlated interconnected bilayer fragments.[16] Pores would open at the beginning of the melting process, forming ruptures at the bilayer surface (a tattered bilayer[19]), which persist up to T_m^{off}. Such spatially correlated fragments would be responsible for the emergence of the SAXS peak at low angles (correlation around 370 Å).

The results shown here give further support to the bilayer perforation model in the transition region. First, MLVs ruptured and disassembled only when entering the transition region, which is a clear sign of bilayer perforation. Second, rupture places at the bilayer surface could be detected when GUVs reached the transition region (see e.g. Figure 4e,j and Figure 5b,e). Third, fluorescence microscopy images shown here confirmed that the lipids that originally formed a vesicle in the fluid phase remained engaged in some structure in the transparent region, giving rise to a blurred and undefined image (see e.g. Figure 4g). A highly perforated and deformed bilayer could well explain such an image, although optical microscopy obviously cannot be conclusive about the lipid assembly in the nanometer length scale. Yet, it is difficult to imagine another lipid assembly that could produce such image that would also (i) maintain the original lipids that once formed the vesicle and (ii) still be mainly a bilayer. The first statement is also sustained by previous experiments that ensure that no lipid exchange between vesicles occurs along the transition region.[14,19] The second argument is supported by ESR and SAXS data. Spin labels at different chain positions (5th−14th carbon) show the typical order/mobility depth profile of bilayers.[17,18] Moreover, a particular probe at the 16th carbon reveals the coexistence of two signals: one consistent with a bilayer and one resembling the signal from a micelle-like environment,[15] which can be interpreted as coming from the pore borders. SAXS data in the transparent region show the presence of the bilayer band, though with a lower electron density contrast than in the gel and fluid phases.[16,17] This evidence can be explained in terms of water inside the pores, which would decrease the electron density contrast of the bilayer.

It is clearer now that for a drastic decrease in the bilayer optical contrast (and dispersion turbidity) to occur, resulting in an almost transparent sample, the water pores should have dimensions comparable to that of the remaining bilayer regions. Small pores can certainly decrease the bilayer contrast, but a transparent sample might only be achieved with extensive bilayer perforation. The model we propose here is similar to the cartoon shown previously,[16] but with the bilayer pieces being further apart and most probably bent and not in the same plane as their neighbors. In this way, a smooth macroscopic surface would vanish and the bilayer would become tattered. However, the bilayer fragments, though in different planes, would be still interconnected, and their typical size/distance would give rise to the correlation peak at 370 Å. The average membrane structure might be achieved from a dynamic bilayer perforation process, in which water pores would be constantly created and destroyed.

In our previous work, we have assumed that "closed" vesicles would still exist in the transparent region, even though with pores/cracks on its surface. However, as pointed out by Alakoskela and Kinnunen 2007,[19] the vesicles most probably open up in the transparent region and become an open sheet. Closed vesicles are normally formed to stabilize the high energy cost of bilayer edges at the expense of the low bending energy, at least in the fluid phase. If bilayer edges are so abundant in the transparent region, closed vesicles might no longer be a requirement. Some ruptures might become so big that the overall bilayer form would be better described as an open deformed sheet. Indeed, we observed several events of open sheets closing to form a vesicle in the fluid phase or vesicles opening up when entering the transition region (see Figure 2 in the Supporting Information). The opening up of vesicles in the transparent region could also explain why no defined closed structure was observed for giant vesicles in the gel phase. Because of the significant resistance to shear and high bending stiffness of bilayers in the gel phase,[29,30] open sheets with micrometer size might not easily reseal in the gel phase.

The extensive perforation proposed seems to explain sample and bilayer transparency, and we propose that this is the preferred lipid assembly in the transparent region. Our data suggest that some level of bilayer perforation extends throughout the whole transition region, also outside the transparent region. From turbidity data, sample turbidity is always lower in the transition region than in the gel and fluid phases, even when it does not reach the transparent level (see Figure 1b for 5−50 mM NaCl). From observations with optical microscopy, we see that many bilayer pieces are not yet closed to form vesicles until T_m^{off} is reached in a heating scan. This suggests that not all pores are closed and the vesicles cannot yet recover its structure. When vesicles are cooled down from the fluid phase, clear morphological changes occur at T_m^{off} (for intermediate salt concentrations, 5−20 mM NaCl), which could only be achieved with an increase in the vesicle area-to-volume ratio. Furthermore, the bilayers clearly become fainter. These observations also suggest the opening of pores across the bilayers. However, in that case pores would not be big and/or extensive enough so as to extinguish the membrane surface in a macroscopic scale, and the optical contrast would still be high

enough so that the bilayer can be seen with optical microscopy, though with a smaller contrast.

We can thus propose that bilayer perforation persists throughout the whole transition region, but the fraction of pores in the total membrane surface changes considerably, and this is an important parameter along the transition region. In the transparent region the fraction of pores is maximal, rendering the bilayer a tattered structure and a defined membrane surface is lost, drastically reducing the bilayer optical contrast. Between T_3 and T_m^{off} pores/ruptures start to close and/or get smaller and molecules that were at the pore borders go to the planar region in the fluid state. Consequently, the fraction of pores in the membrane decreases, and the bilayer contrast and turbidity increase. A complete recovery of contrast/turbidity occurs only when all pores close at T_m^{off}. The fraction of pores should also be sensitive to the concentration of salt, such that the increase in ionic strength reduces the extent of bilayer perforation.

Although the bilayer perforation model can reasonably well explain the specific properties found in the transition region, it remains to understand and explain how such an extensive perforation can exist over such a wide temperature interval. From the one side, it was shown by different approaches that the presence of surface charges can destabilize a bilayer structure.[33−35] From the other side, it is known that small transient pores open at the main transition of lipids,[4−6] which has been termed soft perforation.[6] The opening of pores at the main transition seems to arise because of the increased fluctuations in area and volume per lipid coupled with the fluctuations in enthalpy at the phase transition, which are a function of the excess heat capacity.[31] It would be reasonable to assume that the transition region of DMPG displays this soft perforation coupled with the heat capacity profile. However, the pores observed at the phase transition of lipids are typically small (~10 Å),[6] and none of the properties of the transparent region of DMPG were observed at the phase transition temperature of other lipids. The transparent region is only present with short chain PG lipids at low ionic strength.[13] It has been suggested previously that repulsion among DMPG headgroups in unscreened conditions (pure water) increases the curvature of the hydrophilic interface, thus stabilizing bilayer edges.[10] In a similar way, it was proposed that, due to charge repulsion, DMPG at low ionic strength has a fairly big effective headgroup size.[36] Thus, it is reasonable to expect that the combination of unscreened headgroup charge with short chains gives rise to a lipid with positive curvature. The area fluctuations expected to occur in the melting region could enhance this positive curvature and stabilize bilayer edges, drastically increasing the fraction of pores. Furthermore, the electrostatic repulsion between the bilayer borders could lead to pores/ruptures of sizes on the order of few Debye screening lengths (50 Å in the buffered solution with no added salt) and repulsion among bilayer fragments.

Conclusion

We have studied in detail the transition region of DMPG as a function of the concentration of salt using different techniques. We could establish that the transparent region is smaller than the whole transition region at intermediate concentrations of salt (5−20 mM NaCl for 50 mM DMPG) and finishes at T_3, a new thermal event below T_m^{off}, first identified here and associated with a partial recovery of turbidity and bilayer optical contrast. The transparent region exists only in the presence of up to 20 mM NaCl; yet, a broad transition region, associated with a small decrease in turbidity, persists in the presence of up to 100 mM NaCl. The changes in turbidity could be directly related to the bilayer optical contrast, which we propose to be a consequence of the extent of bilayer perforation. The transparent region seems to be achieved only when pores/ruptures grow and a defined membrane surface vanishes because of repulsion among bilayer fragments. The ionic strength plays a crucial role in pore size/stabilization, and extensive perforation is prevented at sufficiently high ionic strength. The mechanism of bilayer perforation seems to be the coupling of the positive curvature of DMPG, which depends on the ionic strength, with the fluctuations in area in the transition region. We hope the present work will encourage theoretical and simulation studies on how surface charges influence bilayer stability under several circumstances, mainly coupled with lipid melting. This phenomenon might be of biological relevance, as transport across membranes, which contain negatively charged phospholipids, is fundamental for cellular activity.

Acknowledgment. We thank R. Dimova, R. P. Barroso, and C. Haluska for helpful discussions. This work was supported by FAPESP, USP, and CNPq.

Supporting Information Available: Snapshot of the structures obtained in the gel phase (Figure 1); sequence of snapshots showing an open bilayer closing into a giant vesicle at T_m^{off} (up scan) (Figure 2). This material is available free of charge via the Internet at http://pubs.acs.org.

(31) Heimburg, T. *Biochim. Biophys. Acta* **1998**, *1415*, 147–162.
(32) Riske, K. A.; Nascimento, O. R.; Peric, M.; Bales, B.; Lamy-Freund, M. T. *Biochim. Biophys. Acta* **1999**, *1418*, 133–146.
(33) Betterton, M. D.; Brenner, M. P. *Phys. Rev. Lett.* **1999**, *82*, 1598–1601.
(34) Ha, B.-Y. *Phys. Rev. E* **2001**, *64*, 051902.
(35) Shoemaker, S. D.; Vanderlick, T. K. *Biophys. J.* **2002**, *83*, 2007–2014.
(36) Kodama, M.; Miyata, T. *Colloids Surf., A* **1996**, *109*, 283–289.